Available online at www.sciencedirect.com
SCIENCE DIRECT®
Journal of Solid State Chemistry 177 (2004) 3784–3794
JOURNAL OF SOLID STATE CHEMISTRY
www.elsevier.com/locate/jssc

Crystal structure and electrical conductivity of lanthanum–calcium chromites–titanates $La_{1-x}Ca_xCr_{1-y}Ti_yO_{3-\delta}$ ($x=0$–1, $y=0$–1)

V. Vashook[a,*], L. Vasylechko[b], J. Zosel[c], W. Gruner[d], H. Ullmann[a], U. Guth[a,c]

[a]*Institute of Physical Chemistry and Electrochemistry, Dresden University of Technology, D-01062 Dresden, Germany*
[b]*"Lviv Polytechnic" National University, 79013 Lviv, Ukraine*
[c]*Kurt-Schwabe Institute for Measuring and Sensor Technology Meinsberg, D-04720 Ziegra-Knobelsdorf, Germany*
[d]*Leibniz-Institute for Solid State and Materials Research, P.O. Box 270116, D-01171 Dresden, Germany*

Received 21 February 2004; received in revised form 1 July 2004; accepted 9 July 2004
Available online 27 August 2004

Abstract

Five series of perovskite-type compounds in the system $La_{1-x}Ca_xCr_{1-y}Ti_yO_3$ with the nominal compositions $y=0$, $x=0-0.5$; $y=0.2$, $x=0.2-0.8$; $y=0.5$, $x=0.5-1.0$; $y=0.8$, $x=0.6-1.0$ and $y=1$, $x=0.8-1$ were synthesized by a ceramic technique in air (final heating 1350 °C). On the basis of the X-ray analysis of the samples with $(Ca/Ti)\geqslant 1$, the phase diagram of the $CaTiO_3$–$LaCr^{III}O_3$–$CaCr^{IV}O_3$ quasi-ternary system was constructed. Extended solid solution with a wide homogeneity range is formed in the quasi-ternary system $CaCr^{IV}O_3$–$CaTiO_3$–$LaCr^{III}O_3$. The solid solution $La_{(1-x'-y)}Ca_{(x'+y)}Cr^{IV}_{x'}Cr^{III}_{(1-x'-y)}Ti_yO_3$ exists by up to 0.6–0.7 mol fractions of $CaCr^{IV}O_3$ ($x'<0.6-0.7$) at the experimental conditions. The crystal structure of the compounds is orthorhombic in the space group *Pbnm* at room temperature. The lattice parameters and the average interatomic distances of the samples within the solid solution ranges decrease uniformly with increasing Ca content. Outside the quasi-ternary system, the nominal compositions $La_{0.1}Ca_{0.9}TiO_3$, $La_{0.2}Ca_{0.8}TiO_3$, $La_{0.4}Ca_{0.6}Cr_{0.2}Ti_{0.8}O_3$ and $La_{0.3}Ca_{0.7}Cr_{0.2}Ti_{0.8}O_3$ in the system $La_{1-x}Ca_xCr_{1-y}Ti_yO_3$ were found as single phases with an orthorhombic structure. In the temperature range between 850 and 1000 °C, the synthesized single-phase compositions are stable at $pO_2=6\times10^{-16}$–0.21×10^5 Pa. Oxygen stoichiometry and electrical conductivity of the separate compounds were investigated as functions of temperature and oxygen partial pressure. The chemical stability of these oxides with respect to oxygen release during thermal dissociation decreases with increasing Ca-content. At 900 °C and oxygen partial pressure 1×10^{-15}–0.21×10^5 Pa, the compounds with $x>y$ (acceptor doped) are *p*-type semiconductors and those with $x<y$ (donor doped) and $x=y$ are *n*-type semiconductors. The type and level of electrical conductivity are functions of the concentration ratios of cations occupying the *B*-sites of the perovskite structures: $[Cr^{3+}]/[Cr^{4+}]$ and $[Ti^{4+}]/[Ti^{3+}]$. The maximum electrical conductivity at 900 °C and $pO_2=10^{-15}$ Pa was found for the composition $La_{0.1}Ca_{0.9}TiO_3$ (near 50 S/cm) and in air at 900 °C for $La_{0.5}Ca_{0.5}CrO_3$ (close to 100 S/cm).

Keywords: Perovskites; Chromites; Titanates; Crystal structure; Oxygen stoichiometry; Electrical conductivity

1. Introduction

One of the material problems of solid oxide fuel cells (SOFC) for hydrocarbon fuels is the availability of anode materials, which meet simultaneously the requirements of catalytic activity, thermal expansion, and electrical conductivity better than the usually applied Ni/NiO + *YSZ* cermet [1]. Recently, a variety of new compounds were proposed as alternative anode materials for SOFC: $La_{1-x}(Sr,Ca)_xCrO_3$ [1,2], $La_{0.8}Sr_{0.2}Cr_{0.97}V_{0.03}O_3$ [3], $ZrO_2(Y_2O_3+Nb_2O_5)$ [4], $(Sr_{1-x}Ba_x)_{0.6}Ti_{0.2}Nb_{0.8}O_3$ [5], $Gd_2(Ti_{1-y}Mo_y)_2O_7$ [6], $La_{0.6}Sr_{0.4}Co_{0.2}Fe_{0.8}O_3$ [7,8], $La_{1-x}Ba_xCr_{1-y}Ti_yO_{3-\delta}$ [9], and selected compositions in the system $La_{1-x}Ca_xCr_{1-y}Ti_yO_{3-\delta}$ [10]. These materials show a number of disadvantages such as interaction with *YSZ*, insufficient conductivity,

*Corresponding author. Fax: +49-351-463-37752.
E-mail address: vladimir.vashook@chemie.tu-dresden.de (V. Vashook).

0022-4596/$ - see front matter © 2004 Elsevier Inc. All rights reserved.
doi:10.1016/j.jssc.2004.07.007

decomposition under reducing conditions, low thermal expansion, or low catalytic activity. Therefore, the search for new anode materials actually remains, especially with regard to reduced operation temperatures of the SOFC with alternative ceria electrolytes [11].

Complex perovskite-type oxides ABO_3 based on rare earth and alkaline earth oxides with 3d transition metal oxides remain to be interesting candidates for materials with electrocatalytic properties. Lanthanum chromites and titanates substituted with alkaline earth ions are preferred materials of investigation in this field. Mixed occupation of the *B*-site by varying the Cr:Ti ratios enable to modify the donor and acceptor doping. Systematic results on structure, electronic and ionic conductivities as well as catalytic properties of this type of perovskite oxide are not available so far.

Crystal structure, electrical conductivity, oxygen and cation diffusion mobility, and thermodynamic characteristics of doped lanthanum chromites and calcium or strontium titanates are well investigated [12–18]. Only a few results were published in the last few years [10,19–21] on mixed chromites–titanates. Pudmich et al. [10] prepared and investigated a series of lanthanum chromites, partially substituted with alkaline-earth elements in the *A*-position of the perovskite and with transition metals like Ti, Co, or Fe in the *B*-position. A broad range of variations of the physical properties such as electrical conductivity and thermal expansion was observed.

The solubility of Sr in $LaCrO_3$ after [22,23] is relatively small (0.05–0.12 mol), whereas the Ca solubility in analogous chromites reaches 0.5–0.6 mol. Taking into account that the solubility of Ca in chromites is higher than the solubility of Sr, the La–Ca–Cr–Ti–O system was chosen for the investigation of relations between composition, crystal structure and electrical conductivity.

The structural features and conductivity properties of the series $La_{1-x}Ca_xCr_{1-x}Ti_xO_3$ were described in our previous publications [24] ($La_{1-x}Ca_xCr_{0.2}Ti_{0.8}O_3$), [25] ($La_{1-x}Ca_xCr_{0.5}Ti_{0.5}O_3$), [26] ($La_{1-x}Ca_xCr_{0.8}Ti_{0.2}O_3$), and [27] ($La_{1-x}Ca_xTiO_3$). In these works, the crystal structure, oxygen stoichiometry, and electrical conductivity were investigated as functions of the Ca content, oxygen partial pressure and temperature. In this paper we present an overview of the structural and electrical properties of the mixed perovskites in the series $La_{1-x}Ca_xCr_{1-y}Ti_yO_{3-\delta}$ ($x = 0-1$, $y = 0, 0.2, 0.5, 0.8, 1$) together with some new results.

2. Experimental

2.1. Powder preparation and crystal structure investigation

$La_{1-x}Ca_xCr_{1-y}Ti_yO_{3-\delta}$ (x, $y = 0.0-1.0$) powders were prepared by mixing of La_2O_3, $CaCO_3$, Cr_2O_3 and TiO_2 powders with a 99.9% purity. The mixtures were milled in ethanol by means of an agate ball mill for 24 h. After drying the mixtures were heated in air at 1100 °C for 20 h in alumina crucibles. After cooling to room temperature the products were milled again and finally heated in air at 1350 °C for 20 h. The cooling and heating temperature rates during syntheses on these stages were always 5 °C/min. Finally cooled substances were repeatedly milled. Before X-ray and oxygen non-stoichiometry investigations, the powders were treated at 1000 °C for 10 h and cooled to room temperature at a rate of 2 °C/min.

The crystal structures were investigated by means of the powder diffraction technique using a Siemens D5000 powder X-ray diffractometer (Cu*K*α-radiation, $\theta/2\theta$-scanning mode, step width of 0.02°, counting time per step—7 s). The crystal structures were refined by the full-profile Rietveld method, including refinement of lattice parameters, positional and displacement parameters, site occupancy, scaling factor, sample shift, background and Bragg-peak profile parameters. The atomic displacement parameters were refined anisotropically for La(Ca) cations and isotropically for all other atoms. All calculations were performed using the WinCSD (Crystal Structure Determination) program package [28].

2.2. Oxygen content measurements

2.2.1. Initial oxygen content

The oxygen content of the compounds was measured by the carrier gas hot extraction method (CGHE) with a commercial oxygen analyzer TC436-DR (LECO, USA). The powders were weighed (about 25 mg) and filled into a metallic capsule of nickel (0.4 g) with an additional tin tablet (0.2 g). This pressed package was dropped into a degasified high-temperature graphite crucible, which was electrically heated with a power-time-program. Two IR-selective detectors registered simultaneously the formed reaction species CO and CO_2. All values were referred to ZrO_2 measured under the same measurement conditions. A reproducibility of 0.5% RSD can be reached by this method as shown for many oxides by Gruner [29].

Parallel to the CGHE method, the powder samples were analyzed jodometrically after digestion in KJ/HCl solution at elevated temperatures in sealed glass ampoules.

2.2.2. Change of oxygen content

Oxygen content changes were measured by solid-electrolyte technique using the PC-controlled device OXYLYT (SensoTech Magdeburg, Germany) (Fig. 1). The concept of a combined coulometric–potentiometric arrangement for the investigation of interactions between solids and the gaseous environment in the carrier gas mode was described earlier in [30,31].

The amount of oxygen exchanged between the gas flow and a sample within a process in the case of the coulometric method could be determined by the equation

$$\Delta m_{O_2} = k_1 \int_{t=\text{start}}^{t=\text{end}} (I_0 - I_t)\,dt \quad (U_2 = \text{constant}) \tag{1}$$

and in the case of potentiometric method by the equation

$$\Delta m_{O_2} = k_2 \int_{t=\text{start}}^{t=\text{end}} (pO_2^{II} - pO_2^{III})\,dt \quad (I_2 = 0), \tag{2}$$

where k_1 and k_2 are constants, I_0 and I_t are the basic and running titration currents on cell 2, pO_2^{II} and pO_2^{III} are the oxygen partial pressures before and after the reactor, respectively, and t the duration of the process. The constants k_1 and k_2 consider the gas flow rate, temperature of the gas flow meter, and the electrochemical equivalent of oxygen.

Oxygen partial pressures (pO_2) in the reactor are calculated by the Nernst-equation for $pO_2 > 0.1$ Pa

$$U = \frac{RT}{4F} \ln \frac{pO_2}{pO_2^{air}}, \tag{3}$$

where U is the voltage of the solid electrolyte cell, R the absolute gas constant, T the absolute temperature of the electrochemical cell, and F the Faraday constant and pO_2^{air} the oxygen partial pressure in air. In atmospheres with strongly reduced oxygen partial pressures, as for example, $Ar/H_2/H_2O$ mixtures, the oxygen partial pressure in the reactor could be calculated by the following equation:

$$pO_2 = k_3^2 \left(\frac{pH_2O}{pH_2}\right)^2, \tag{4}$$

where k_3 is the constant of the water dissociation reaction ($2H_2O \rightleftharpoons 2H_2 + O_2$), pH_2O and pH_2 are the water vapour and hydrogen partial pressures in the gas stream, respectively.

The investigation of oxygen non-stoichiometry was performed on powder samples prepared as described in Section 2.1. Air, Ar/O_2, and $Ar/H_2/H_2O$ were used as the initial reaction gas mixtures with the defined oxygen partial pressures 21000, 1 Pa and $pH_2O/pH_2 = 0.01$, respectively. The electrical conductivities were measured on ceramic bars with rectangular cross section, which were placed in the reactor at controlled temperatures and oxygen partial pressures. The observed accuracy of changes of the oxygen content was better than ± 0.005 of oxygen atomic index.

2.3. Electrical conductivity measurements

The electrical conductivity (σ) of ceramic samples was measured in gas atmospheres with defined oxygen partial pressures (Fig. 1) by a DC four-point method described elsewhere [32]. The powders were pressed into shapes of $1 \times 3 \times 10\,mm^3$ together with 4 Pt wires (0.1 mm by diameter) and sintered for 20 h in air at temperatures of 1250–1400 °C depending on composition. Heating and cooling rates during sintering were 5 °C/min. The conductivity was measured at 20–1000 °C in air and in flowing gas mixtures of Ar/O_2 (1–100 Pa O_2) and $Ar/H_2/H_2O$ with $pH_2O/pH_2 = 0.01$–50. Equilibrium state values of the conductivity at 900 °C and different oxygen partial pressures were achievable after 1–100 h of exposition depending on oxygen partial pressure range, composition and ceramic structure of the samples. The temperature dependencies of the electrical conductivity in air and in gas flow of $Ar/H_2O/H_2$ with $pH_2O/pH_2 = 0.01$ were recorded during cooling at a rate of 5 °C/min.

3. Results and discussion

3.1. Synthesis and crystal structure of the compounds in the system $La_{1-x}Ca_xCr_{1-y}Ti_yO_3$

The phase compositions of the samples obtained after synthesis in air at 1350 °C are given in Table 1. Single-phase samples occur mostly for the compositions with

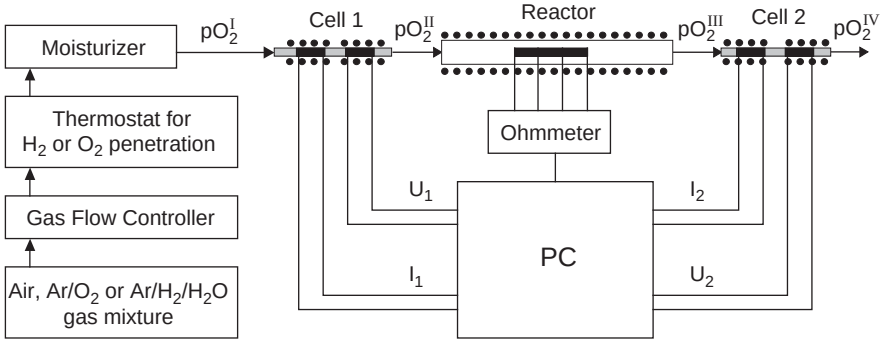

Fig. 1. Scheme of the solid electrolyte device oxylyt for solid-state coulometry and electrical conductivity measurements.

$x \geqslant y$. The samples with nominal compositions $La_{0.1}Ca_{0.9}TiO_3$, $La_{0.2}Ca_{0.8}TiO_3$, $La_{0.4}Ca_{0.6}Cr_{0.2}Ti_{0.8}O_3$ and $La_{0.3}Ca_{0.7}Cr_{0.2}Ti_{0.8}O_3$ (all with $x<y$) were found to be single-phase compositions too, according to the results of the X-ray phase analysis.

Decreasing x/y ratios at some values led to the appearance of non-perovskite phases, mainly the oxygen intergrowth phases of the type $La_n(Ti,Cr)_nO_{3n+2}$ [33] (Table 1). The amount of $La_n(Ti,Cr)_nO_{3n+2}$ phases increase and the perovskite phases diminish with decreasing x/y ratio, respectively.

There are two distinct ranges of the $La_{1-x}Ca_xCr_{1-y}Ti_yO_3$ system, depending on two different modes of charge compensation at La–Ca substitution as shown in [24–27]. For $La_{1-x}Ca_xCr_{1-y}Ti_yO_3$ with $x \geqslant y$, the compensation of negative charges at the partial substitution of La^{3+} with Ca^{2+} is based on the change of the chromium oxidation states. In contrast to that mode, at $x<y$ the oxidation levels of chromium (3+) and titanium (4+) cations stay unchanged and the charge compensation is based on the formation of cation vacancies. Precipitation of non-perovskite phases occurs in the $La_{1-x}Ca_xCr_{1-y}Ti_yO_3$ system at $x<y$ when $y = 0.2-0.5$ and at $x<(y-0.2)$ when $y = 0.8-1.0$.

The phase diagram of the quasi-ternary system $CaCr^{IV}O_3$–$CaTiO_3$–$LaCr^{III}O_3$ was constructed on the basis of X-ray phase and structural analysis of the $La_{1-x}Ca_xCr_{1-y}Ti_yO_3$ samples with $x \geqslant y$ (Fig. 2). Extended solid solutions with a wide homogeneity range are formed in this system at 1350 °C in air. The formation of these solid solutions is not surprising because all three end-members of the system ($LaCrO_3$, $CaTiO_3$ and $CaCrO_3$) adopt the same $GdFeO_3$-type structure. Continuous solid solution is formed in the $CaTiO_3$–$LaCrO_3$ pseudo-binary system (Fig. 3a). The third end-member on the system ($CaCr^{IV}O_3$) could be obtained by a solid-state reaction only by application of high-pressure synthesis (65 kbar at 700 °C) [34]. Therefore, the solid solution ranges in the pseudo-binary systems $CaTiO_3$–$CaCr^{IV}O_3$ and $LaCr^{III}O_3$–$CaCr^{IV}O_3$ (Figs. 3b and c) and in the quasi-ternary system $CaCr^{IV}O_3$–$CaTiO_3$–$LaCr^{III}O_3$ (Fig. 2) do not exceed ~60–70 molar percent of $CaCr^{IV}O_3$ at the ambient conditions mentioned above. Besides the $La_{(1-x'-y)}Ca_{(x'+y)}Cr^{IV}_{x'}Cr^{III}_{(1-x'-y)}Ti_yO_3$ perovskite-like compounds, $Ca_2Cr_2O_5$ and $CaCr_2O_4$ are formed in the $CaCr^{IV}O_3$-rich corner of the phase diagram.

All the single-phase compounds in the $LaCr^{III}O_3$–$CaTiO_3$–$CaCr^{IV}O_3$ system show the orthorhombically distorted $GdFeO_3$-type structure. Fig. 4 summarizes the lattice parameters and cell volumes of the samples within the $La_{1-x}Ca_xCr_{1-y}Ti_yO_3$ solid solution region. The corresponding values for $CaCrO_3$ obtained by

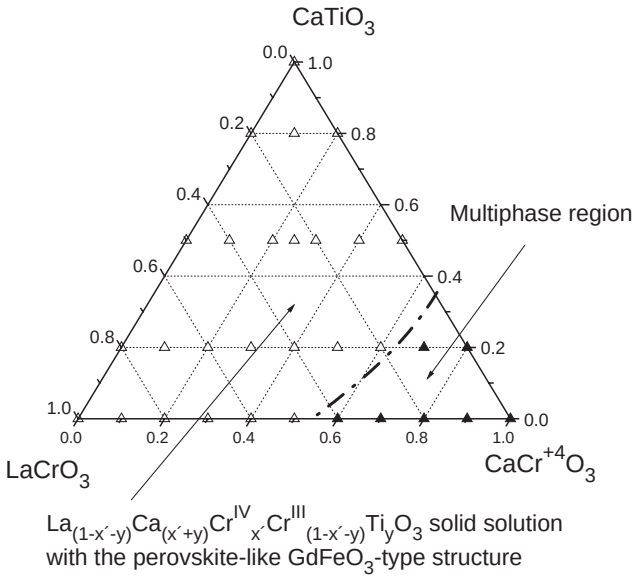

Fig. 2. Range of existence of the perovskite-like phases in the system $La_{1-x}Ca_xCr_{1-y}Ti_yO_3$.

Table 1
Composition and structure of compounds in the series $La_{1-x}Ca_xCr_{1-y}Ti_yO_3$

Series	x	Phases
$La_{1-x}Ca_xCrO_3$	$0 \leqslant x \leqslant 0.5$	Perovskite
$La_{1-x}Ca_xCr_{0.8}Ti_{0.2}O_3$	$x = 0, 0.1$	Perovskite (~95–97%) + unknown phase (~3–5%)
	$0.2 \leqslant x \leqslant 0.8$	Perovskite
	$x = 0.9$	Perovskite + $Ca_2Cr_2O_5$ (~30%)
	$x = 1$	Perovskite (~50%) + $Ca_2Cr_2O_5$ (~11%) + $Ca(CrO_2)_2$ (~25%) + $Ca_3(CrO_4)_2$ (~8%)
$La_{1-x}Ca_xCr_{0.5}Ti_{0.5}O_3$	$x = 0, 0.1$	Perovskite (70–77%) + $La_5(Ti,Cr)_5O_{17}$ (10–8%) + $La_2Ti_2O_7$ (14–10%) + $La_5(Ti,Cr)_4O_{15}$ (6–5%)
	$0.2 \leqslant x \leqslant 0.4$	Perovskite (90–97%) + $CaLa_4Ti_5O_{17}$ (10–3%)
	$0.5 \leqslant x \leqslant 1$	Perovskite
$La_{1-x}Ca_xCr_{0.2}Ti_{0.8}O_3$	$0.2 \leqslant x \leqslant 0.5$	Perovskite + $La_5Ti_5O_{17}$ (30–10%)
	$0.6 \leqslant x \leqslant 1$	Perovskite
$La_{1-x}Ca_xTiO_3$	$x = 0.2$	$CaLa_4Ti_5O_{17}$ (80–90%) + perovskite (10–15%)
	$x = 0.3$	$Ca_2La_4Ti_6O_{20}$ (~70%) + perovskite (20–25%) + $CaLa_4Ti_5O_{17}$ (5–10%)
	$0.4 \leqslant x \leqslant 0.7$	Perovskite (75–95%) + $Ca_2La_4Ti_6O_{20}$ (5–25%)
	$0.8 \leqslant x \leqslant 1$	Perovskite

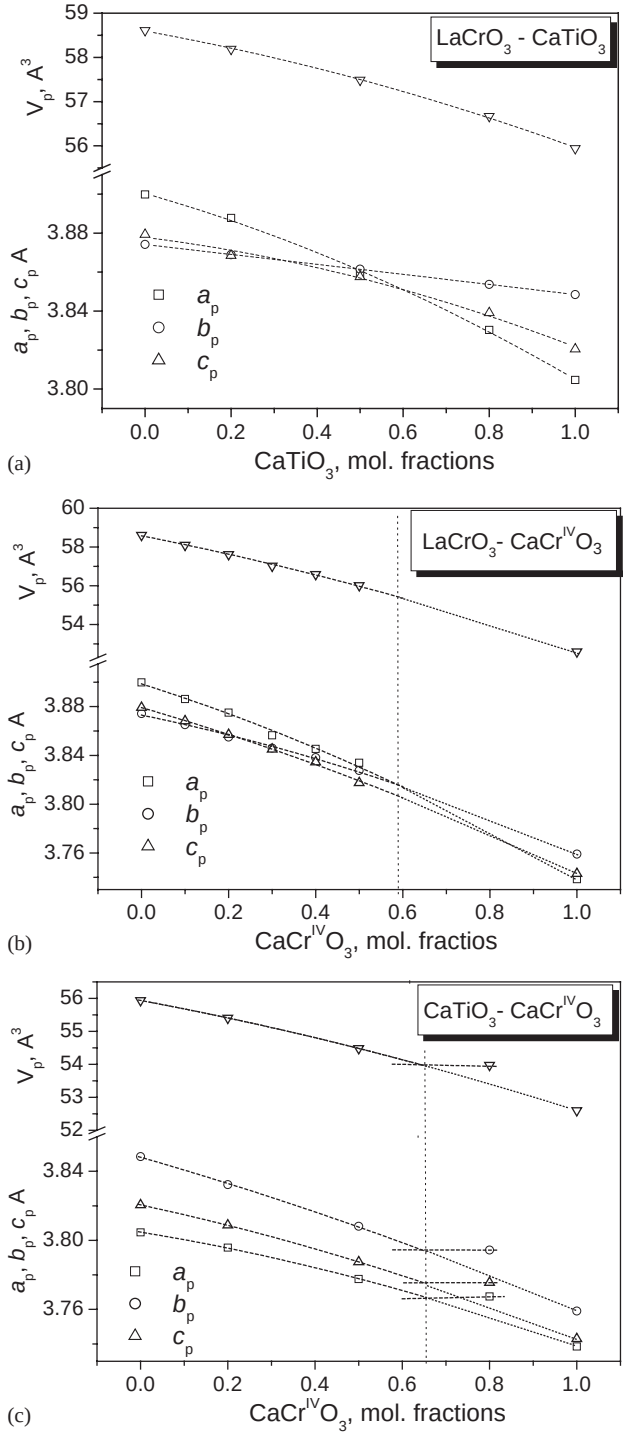

Fig. 3. Compositional dependencies of the lattice parameters and cell volumes in the pseudo-binary systems $LaCrO_3$–$CaTiO_3$ (a), $LaCrO_3$–$CaCrO_3$ (b) and $CaTiO_3$–$CaCrO_3$ (c), orthorhombic lattice parameters are transformed into the perovskite-like cell parameters as follows: $a_p=a_0/\sqrt{2}$, $b_p=b_0/\sqrt{2}$, $c_p=c_0/2$, $V_p = V_0/4$, cell parameters of $CaCrO_3$, obtained by solid-state reaction at 65 kbar and 700 °C, were taken from [34].

solid-state reaction at 65 kbar and 700 °C [34] are given additionally for comparison. Fig. 5 represents the average interatomic distances between the atoms in the first coordination sphere of the investigated structures. Lattice parameters and interatomic distances in the $La_{1-x}Ca_xCr_{1-y}Ti_yO_3$ compounds change uniformly with composition, in accordance with average radii of *A*- (due to substitution of Ca for La) and *B*-cations (due to substitution of Ti for Cr and partial reduction of Cr^{4+} to Cr^{3+}). All structural parameters of compositions within the solid solution range are placed in the triangle $CaTiO_3$–$LaCrO_3$–$CaCrO_3$ (Figs. 4 and 5). This result together with the compositional dependencies of the lattice parameters and average interatomic distances prove clearly the existence of extended solid solution with the perovskite-like structure in the quasi-ternary $LaCr^{III}O_3$–$CaTiO_3$–$CaCr^{IV}O_3$ system.

The determined oxygen contents of some selected compounds in the system $La_{1-x}Ca_xCr_{0.5}Ti_{0.5}O_{3-\delta}$, measured by CGHE, are presented in Table 2 together with the calculated nominal oxygen contents according to the formulas, the average values (AVG) of oxygen contents, the standard deviations (SD) of the series of 4–5 measurements, in some cases the reproduction of the measurement series (RSD) and the oxygen contents pro-perovskite unit. The methodical ability has been proofed by two commercial titanates from ChemPur (Germany). For pure $BaTiO_3$ (99.9 wt%) the experimental value corresponds with the expected stoichiometries with acceptable reproducibility. The poor accuracy in the case of $CaTiO_3$ (99 wt%) cannot be understood and may be attributed to other components not certified in detail by the producer. For single-phase compounds like $La_{0.3}Ca_{0.7}Cr_{0.5}Ti_{0.5}O_3$, the oxygen content was analyzed according to the stoichiometric formula with a relative good precision. But higher discrepancies of experimental results and nominal values of oxygen content in the case of $La_{0.4}Ca_{0.6}Cr_{0.5}Ti_{0.5}O_3$ and $La_{0.5}Ca_{0.5}Cr_{0.5}Ti_{0.5}O_3$ powders cannot be explained, as in the case of commercial $CaTiO_3$. More precise and reproducible results were obtained by iodometry. These were used as initial oxygen contents for the further investigations of oxygen non-stoichiometry (Table 3 and Fig. 7).

3.2. Electrical conductivity and oxygen non-stoichiometry

The typical pO_2-dependencies of the electrical conductivity for the single-phase ceramic samples in the system $La_{1-x}Ca_xCr_{1-y}Ti_yO_{3-\delta}$ at 900 °C are presented in Fig. 6. The first group of the compounds ($x/y>1$) shows the *p*-type conductivity. The slope k of the log $(\sigma) = k\log(pO_2)$ dependences for $La_{0.1}Ca_{0.9}Cr_{0.2}Ti_{0.8}O_3$ [24] and $La_{0.4}Ca_{0.6}Cr_{0.5}Ti_{0.5}O_3$ [25] amounts to $k = +1/4$ in the range $pO_2 < 10^{-5}$ Pa and to $k \approx 0$ at more oxidizing conditions. The single-phase samples of the second group of the compounds with $x/y<1$ are *n*-type semiconductors with $k = -1/4$ in the whole pO_2 range from 10^{-15} to 10^5 Pa. The compounds

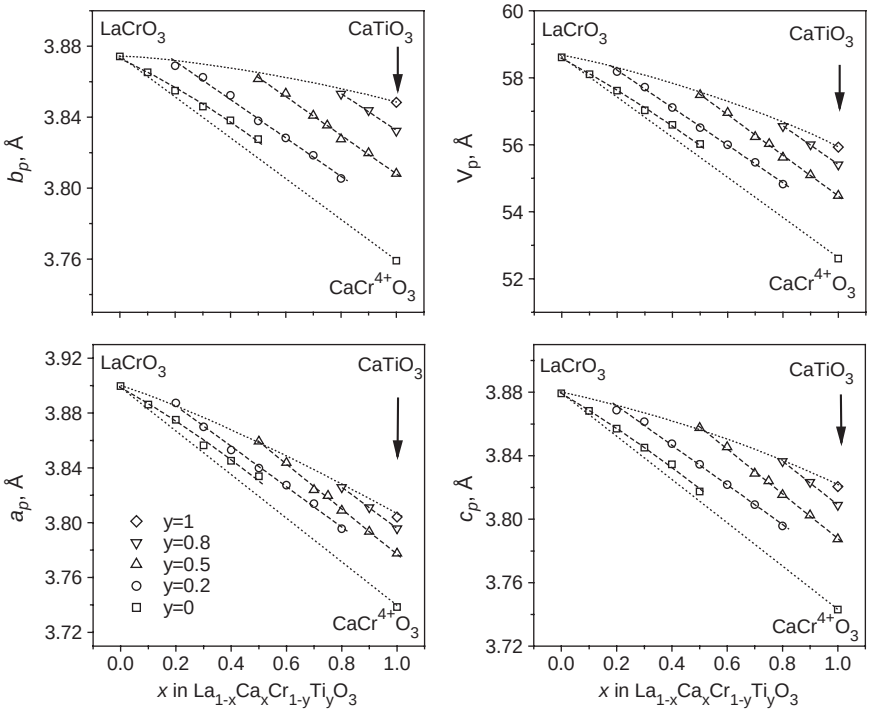

Fig. 4. Lattice parameters of the $La_{1-x}Ca_xCr_{1-y}Ti_yO_3$ samples with perovskite-like structure ($x \geqslant y$), transformation of orthorhombic lattice parameters into perovskite-like cell parameters and cell parameters of $CaCrO_3$ see Fig. 3.

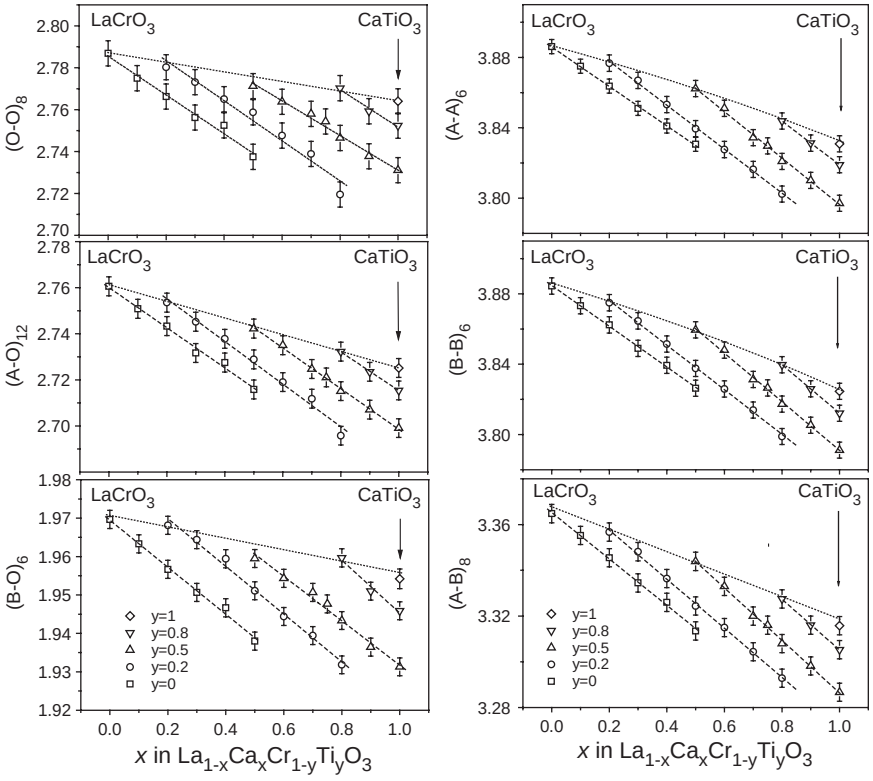

Fig. 5. Average interatomic distances of the $La_{1-x}Ca_xCr_{1-y}Ti_yO_3$ samples with $x \geqslant y$ within the solid solution range with perovskite-like structure.

with $x \approx y$ demonstrate the change from *n*-type conductivity with $k = -1/4$ to *p*-type conductivity with $k = +1/4$ near the conductivity minima. Similar to the compositions with $x > y$ they show weak log (σ) versus log (pO_2) dependencies with $k \approx 0$ at high pO_2.

Table 2
Results of the chemical analysis of some of the powder samples in the system $La_{1-x}Ca_xCr_{1-y}Ti_yO_3$ by means of the carrier gas hot extraction method (CGHE) and iodometry

Formula	Oxygen content, wt%			RSD	Oxygen content pro perovskite unit	
	Nominal	AVG	SD		CGHE	Iodometry
$La_{0.3}Ca_{0.7}Cr_{0.5}Ti_{0.5}O_3$	28.63	28.39	0.22	0.8	2.98±0.02	2.99±0.01
		28.37	0.19	0.7		
		28.50	0.09	0.3		
$La_{0.4}Ca_{0.6}Cr_{0.5}Ti_{0.5}O_3$	27.03	26.46	0.41	1.5	2.94±0.04	2.99±0.01
$La_{0.5}Ca_{0.5}Cr_{0.5}Ti_{0.5}O_3$	25.61	25.30	0.36	1.4	2.96±0.04	2.99±0.01
		25.32	0.64	2.5		
		25.08	0.69	2.8		
$BaTiO_3$ (Commercial)	20.58	20.64	0.04	0.2	3.00±0.006	2.99±0.01
$CaTiO_3$ (Commercial)	35.30	32.28	1.18	3.6	2.74±0.1	2.99±0.01

AVG, average value of oxygen content; SD, standard deviation of the results from 4 to 5 measurements; RSD, reproducibility of measurement series.

Table 3
Oxygen atomic indices of the single-phase $La_{1-x}Ca_xCr_{1-y}Ti_yO_{3-\delta}$ compounds with $x \geqslant y$ at room temperature in air and in $Ar/H_2/H_2O$ gas flow ($pO_2 = 8 \times 10^{-11}$ Pa) at 1000 °C

NN	x	y	3-δ' RT air	3-δ'1000 °C $Ar/H_2/H_2O$	NN	x	y	3-δ' RTair	3-δ' 1000 °C $Ar/H_2/H_2O$
1	0	0	2.99	3.0	14	0.5	0.5	2.99	2.95
2	0.1	0	2.99	2.98	15	0.6	0.5	2.99	2.92
3	0.2	0	2.99	2.94	16	0.7	0.5	2.99	2.90
4	0.3	0	2.99	2.90	17	0.8	0.5	2.99	2.85
5	0.4	0	2.99	2.87	18	0.9	0.5	2.99	2.82
6	0.5	0	2.99	2.81	19	1.0	0.5	2.99	2.77
7	0.2	0.2	2.99	2.99	20	0.8	0.8	2.99	2.97
8	0.3	0.2	2.99	2.99	21	0.9	0.8	2.99	2.96
9	0.4	0.2	2.99	2.97	22	1.0	0.8	2.99	2.90
10	0.5	0.2	2.99	2.94					
11	0.6	0.2	2.99	2.90					
12	0.7	0.2	2.99	2.77	23	0.9	1.0	2.99	2.96
13	0.8	0.2	2.99	2.60	24	1.0	1.0	2.99	2.98

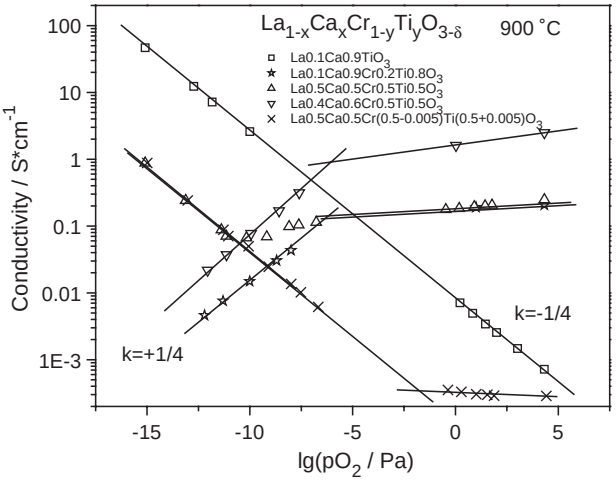

Fig. 6. pO_2 dependencies of the electrical conductivity for some ceramics in the system $La_{1-x}Ca_xCr_{1-y}Ti_yO_{3-\delta}$ at 900 °C.

As an example, the changing titration currents in cell 2 and the corresponding calculated oxygen atomic indexes of $La_{1-x}Ca_xCrO_{3-\delta}$ during heating, exposition and cooling in a gas flow $Ar/H_2/H_2O$ with $pH_2O/pH_2 = 0.53$ are shown in Fig. 7. Analogous dependencies for the other series were given previously in [24–27]. The exposition at 1000 °C during 1 h was sufficient to reach the equilibrium states of the fine-powdered single-phase samples at the conditions mentioned above. The increasing Ca content of $La_{1-x}Ca_xCrO_{3-\delta}$ results in decreasing stability of the compounds with respect to thermal dissociation with oxygen release. No oxygen release was observed for $LaCrO_3$ up to 1000 °C.

The thermal stability of the series $La_{1-x}Ca_xCr_{0.8}Ti_{0.2}O_{3-\delta}$ [26], $La_{1-x}Ca_xCr_{0.5}Ti_{0.5}O_{3-\delta}$ [25], and $La_{1-x}Ca_xCr_{0.2}Ti_{0.8}O_{3-\delta}$ [24] decreases with increasing Ca/Ti ratio. The compounds with the Ca/Ti = 1 ratio do not change their oxygen content during heating from

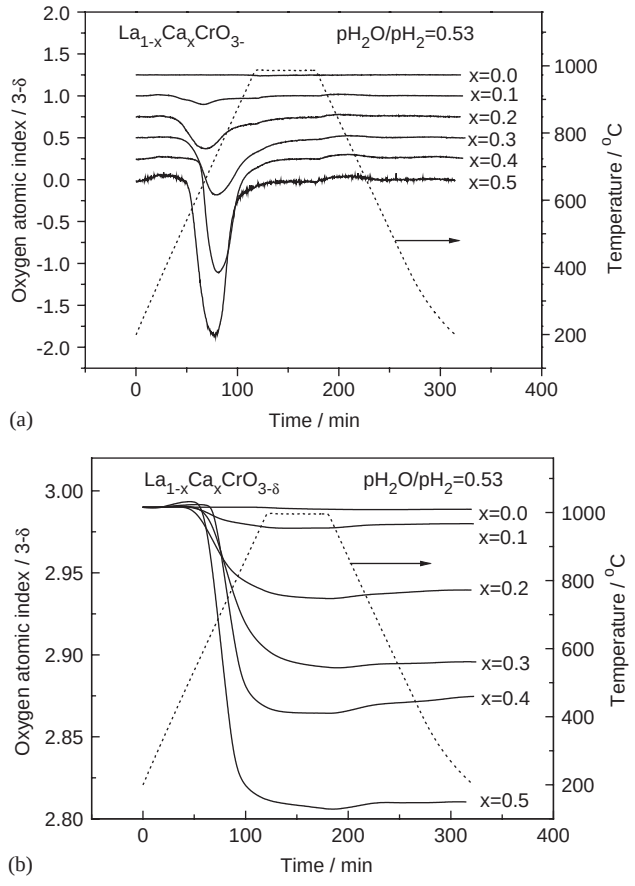

Fig. 7. Oxygen exchange characteristics of the powder samples $La_{1-x}Ca_xCrO_{3-\delta}$ during heating and cooling in $Ar/H_2/H_2O$ ($pH_2O/pH_2=0.53$): (a) titration current of the coulometric cell, and (b) calculated oxygen atomic index (3δ).

room temperature to 1000 °C in gas flows with $pO_2>1$ Pa and show only small oxygen releases in reducing atmospheres.

The oxidation state of Ti cations in this system is most likely constant and amounts to 4+ under oxidizing conditions (near air), whereas Cr cations can change their oxidation state between 3+ and 4+ depending on the Ca/Ti ratios. At increasing temperatures or at reducing conditions firstly chromium cations change their oxidation states from 4+ to 3+, followed by titanium cations. The $La_{1-x}Ca_xCrO_{3-\delta}$ compounds with $x>y$ prepared in air show black color due to the presence of Cr^{4+} cations. The intensity of black color increases with rising Cr^{4+} and Cr^{3+} cation content. The single-phase powders of the series with $x<y$ are light yellow after synthesis in air, but these turn into black color after annealing at reducing conditions due to the appearance of Ti^{3+} cations.

Increasing Ca content at a constant Cr/Ti ratio as well as increasing Cr content at a constant Ca/La ratio are accompanied with increasing amounts of Cr^{4+} cations in the compounds with $x>y$ prepared in air. During heating at reducing conditions the oxygen release increases with rising Cr^{4+} content.

Oxygen release of the $La_{1-x}Ca_xCr_{1-y}Ti_yO_3$ series with $x>y$ can be explained firstly with the reduction of Cr^{4+} cations and then with the following reduction of Ti^{4+} cations at more reducing conditions:

$$La^{3+}_{1-x}Ca^{2+}_{x}Cr^{3+}_{1-x}Cr^{4+}_{x-y}Ti^{4+}_{y}O_3 \rightleftharpoons La^{3+}_{1-x}Ca^{2+}_{x}Cr^{3+}_{1-x+2\delta}Cr^{4+}_{x-y-2\delta}Ti^{4+}_{y}O_{3-\delta}+\frac{\delta}{2}O_2 \quad (5)$$

$$La^{3+}_{1-x}Ca^{2+}_{x}Cr^{3+}_{1-x+2\delta}Cr^{4+}_{x-y-2\delta}Ti^{4+}_{y}O_{3-\delta}+\frac{\delta}{2}O_2 \rightleftharpoons La^{3+}_{1-x}Ca^{2+}_{x}Cr^{3+}_{1-x+2\delta}Cr^{4+}_{x-y-2\delta}Ti^{4+}_{y-2\gamma}Ti^{3+}_{2\gamma}O_{3-\delta-\gamma}+\frac{\delta+\gamma}{2}O_2 \quad (6)$$

The heating of individual lanthanum–calcium titanates [27] and chromites (Fig. 7) in reducing gas flows is accompanied with only one maximum of oxygen release, whereas mixed lanthanum–calcium titanate–chromites show two oxygen release maxima, as is the case for $La_{0.2}Ca_{0.8}Cr_{0.8}Ti_{0.2}O_3$ [26], for example. The maximum at lower temperature corresponds evidently with the reduction of Cr^{4+} to Cr^{3+} according to Eq. (5) and the second maximum comes with the reduction of Ti^{4+} to Ti^{3+}, described by Eq. (6). The contribution of the Ti^{4+} cations to the oxygen release is small in comparison with that of the Cr^{4+} cations. In some cases, only one maximum is observed, because the temperature positions of the separate maxima are influenced by the cationic compositions, oxygen exchange rates, oxygen diffusion mobilities, and dispersion of the powders.

The relatively high stability of $LaCrO_3$ can be explained with the absence of reducible cations at the applied conditions (Fig. 7). The La chromites partially substituted with Ca can release oxygen according to the following equation:

$$La^{3+}_{1-x}Ca^{2+}_{x}Cr^{3+}_{1-x}Cr^{4+}_{x}O_3 \rightleftharpoons La^{3+}_{1-x}Ca^{2+}_{x}Cr^{3+}_{1-x+2\delta}Cr^{4+}_{x-2\delta}O_{3-\delta}+\frac{\delta}{2}O_2 \quad (7)$$

The equilibrium oxygen atomic indexes of the $La_{1-x}Ca_xCr_{1-y}Ti_yO_{3-\delta}$ compounds with $x\geqslant y$ and $y=0$, 0.2, 0.5, 0.8 and 1.0 at 1000 °C and $pO_2\approx 8\times10^{-11}$ Pa ($pH_2O/pH_2=0.53$) are presented in Table 3.

The existence of the single-phase donor-doped compounds with the nominal formula $La_{1-x}Ca_xCr_{1-y}Ti_yO_3$ ($x<y$) can be understood either by formation of cation vacancies $(La_{1-x}Ca_xCr_{1-y}Ti_y)_{6/(6-x+y)2(y-x)/(6-x+y)}O_3$, or by oxygen interstitials according to the formula $La_{1-x}Ca_xCr_{1-y}Ti_yO_{3+(y-x)/2}$. The second possibility is unlikely because it contradicts the general structural concept of perovskites and the results of structural investigations of $La_{1-x}Ca_xCr_{1-y}Ti_yO_3$ (Section 3.1).

The chemical formula of the donor-doped compounds ($x<y$) is assumed as $(La_{1-x}Ca_xCr_{1-y}Ti_y)_{6/(6-x+y)}O_3$, because no impurities of other compounds were registered. It may be that cation vacancies are statistically distributed in the cationic sub-lattice. Oxygen release of these compositions at increasing temperatures and low pO_2 can be described with the following equation:

$$(La^{3+}_{1-x}Ca^{2+}_{x}Cr^{3+}_{1-y}Ti^{4+}_{y})_{6/(6-x+y)}O_3 \rightleftharpoons \frac{6}{6+\delta(6-x+y)} \cdot (La^{3+}_{1-x}Ca^{2+}_{x}Cr^{3+}_{1-y}Ti^{4+}_{y-\gamma}Ti^{3+}_{\gamma})_{(6/(6-x+y))+\gamma}O_3 + \frac{3\gamma(6-x+y)}{12+2\gamma(6-x+y)} \cdot O_2 \quad (8)$$

During the reduction of these oxygen stoichiometric compositions, Ti^{3+} cations are formed due to the simultaneous removal of oxygen ions and metal vacancies. Only a very small oxygen release was registered during heating of the $(La_{1-x}Ca_xCr_{1-y}Ti_y)_{6/(6-x+y)}O_3$ powders with $x<y$ at reducing conditions. That behavior was also found for the $La_{1-x}Ca_xCr_{1-y}Ti_yO_3$ compounds with $x \approx y$.

A weak dependency of the electrical conductivity of $La_{1-x}Ca_xCr_{1-y}Ti_yO_3$ with $x>y$ versus oxygen partial pressure at $pO_2>10^{-5}$ Pa (Fig. 6) indicates stability of these compounds with respect to oxygen release after Eq. (5). The p-type conductivity with $k=+1/4$ in the more reducing region corresponds with decreasing concentration of Cr^{4+} cations (holes) of these compounds with oxygen release. From Eq. (5) and the mass action law follows $[Cr^{4+}]=\text{const}\times pO_2^{+1/4}$, if the concentration of $La_{1-x}Ca_xCr^{3+}_{1-x}Cr^{4+}_{x-y}Ti^{4+}_yO_3$ could be assumed as constant. The same dependence was found for $La_{1-x}Sr_xCrO_{3-\delta}$, in [35], for example. The observed p-type conductivity with $k=+1/4$ indicates that no Ti^{3+} cations are simultaneously formed (Eq. (6)) by decreasing pO_2 up to 10^{-15} Pa (Fig. 6).

The n-type conductivity of $(La^{3+}_{1-x}Ca^{2+}_xCr^{3+}_{1-y}Ti^{4+}_y)_{6/(6-x+y)}O_3$ with $x<y$ (Fig. 6) correlates with increasing concentration of Ti^{3+} cations according to oxygen release after Eq. (8). The $La_{0.1}Ca_{0.9}TiO_3$ (Fig. 6) and $La_{0.2}Ca_{0.8}TiO_3$ [27] ceramic samples at 900 °C show ideal linear dependencies in the range $pO_2=10^{-15}$ … 10^5 Pa. Other donor-doped chromites–titanates $(La^{3+}_{1-x}Ca^{2+}_xCr^{3+}_{1-y}Ti^{4+}_y)_{6/(6-x+y)}O_3$ show small deviations from linear dependencies only in the region of high oxygen partial pressures. An explanation of the observed $\log(\sigma)=k\log(pO_2)^{-1/4}$ dependencies for the compounds in the similar $La_{1-x}Ba_xCr_{1-y}Ti_yO_{3-\delta}$ system with $x<y$ ($0.0<x<0.2$ and $0.0<y<0.5$) at temperatures between 800 and 1000 °C and $pO_2=10^{-15}$–10^5 Pa was given in [9]. Cation vacancies have to be assumed as the predominant point defects in $La_{1-x}Ca_xCr_{1-y}Ti_yO_3$, if $x<y$ and La, Ca, Cr, Ti and O have constant oxidation states 3+, 2+, 3+, 4+, and 2−, respectively. It was shown that conductivity of $La_{1-x}Ba_xCr_{1-y}Ti_yO_{3-\delta}$ is directly proportional to $pO_2^{-1/4}$, if Ti^{4+} is far from being completely reduced to Ti^{3+}.

The minima of conductivity versus oxygen partial pressure observed for some compounds with $x \approx y$, as, for example, $La_{0.2}Ca_{0.8}Cr_{0.2}Ti_{0.8}O_3$ [24] and $La_{0.5}Ca_{0.5}Cr_{0.5}Ti_{0.5}O_3$ (Fig. 6) can be explained evidently with minor deviations from the cationic compositions strived for with the solid-state synthesis. If the ratio of x/y amounts to 1.001 in $La_{1-x}Ca_xCr_{1-y}Ti_yO_3$, the corresponding $(x-y)$ amount of Cr^{4+} cations should exist in the compound. Evidently these tiny fractions of Cr^{4+} cations provide the p-type conductivity with $k=+1/4$ in the pO_2-rich region beside the minimum (Fig. 6) corresponding to Eq. (5). The n-type conductivity at the pO_2 poor region beside the minimum can be provided by increasing concentration of Ti^{3+} cations according to Eq. (6). That dependence of the conductivity from pO_2 corresponds with two maxima of oxygen release, observed during programmed heating of the compounds with $x \approx y$ in reducing atmosphere [24,25], when the concentration of Cr^{4+} cations in the prepared compound is comparable with the concentration of formed Ti^{3+} cations during oxygen release. Actually, the compound with the nominal composition $La_{0.5}Ca_{0.5}Cr_{0.5-0.005}Ti_{0.5+0.005}O_3$ showed linear $\log(\sigma)=k\log(pO_2)^{-1/4}$ dependence (Fig. 6) in contrast to $La_{0.5}Ca_{0.5}Cr_{0.5}Ti_{0.5}O_3$. Evidently, in compounds where x equals y exactly, the following reduction reaction takes place:

$$La^{3+}_{1-x}Ca^{2+}_xCr^{3+}_{1-y}Ti^{4+}_yO_3 \rightleftharpoons La^{3+}_{1-x}Ca^{2+}_xCr^{3+}_{1-y}Ti^{4+}_{y-2\gamma}Ti^{3+}_{2\gamma}O_{3-\gamma}+\frac{\gamma}{2}O_2 \quad (9)$$

The temperature dependencies of the electrical conductivity measured in air during cooling with a rate of 6 °C/min showed semi-conducting types for all single-phase samples of the system $La_{1-x}Ca_xCr_{1-y}Ti_yO_{3-\delta}$ (Fig. 8). The electrical conductivity increases systematically with increasing Cr content. The dependencies of the electrical conductivity from the Ca-content for single-phase ceramic samples in the system $La_{1-x}Ca_xCr_{1-y}Ti_yO_{3-\delta}$ at 1000 °C in air have maxima at $x=0.5$ for $La_{1-x}Ca_xCrO_{3-\delta}$, $x=0.6$ for $La_{1-x}Ca_xCr_{0.8}Ti_{0.2}O_{3-\delta}$, $x=0.75$ for $La_{1-x}Ca_xCr_{0.5}Ti_{0.5}O_{3-\delta}$, and $x=0.95$ for $La_{1-x}Ca_xCr_{0.2}Ti_{0.8}O_{3-\delta}$, (Fig. 9). These dependencies correlate with the dependencies of the product of the molar concentration of Cr^{3+} and Cr^{4+} cations, assuming that the oxygen indexes of the investigated chromites–titanates amount to 3.0 and the oxidation state of Ti cations is 4+. Consequently, the conductivity values of the $La_{1-x}Ca_xCr_{1-y}Ti_yO_{3-\delta}$ compounds with $x>y$ correlate with the exchange intensity of electrons between

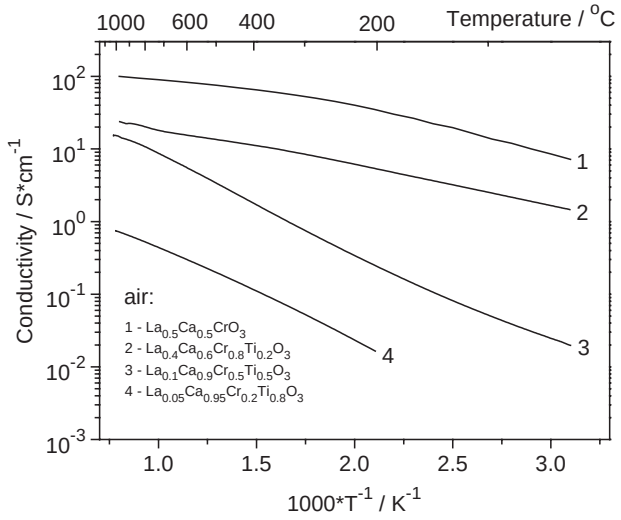

Fig. 8. Temperature dependencies of the electrical conductivity of ceramic samples in the system $La_{1-x}Ca_xCr_{1-y}Ti_yO_{3-\delta}$ in air.

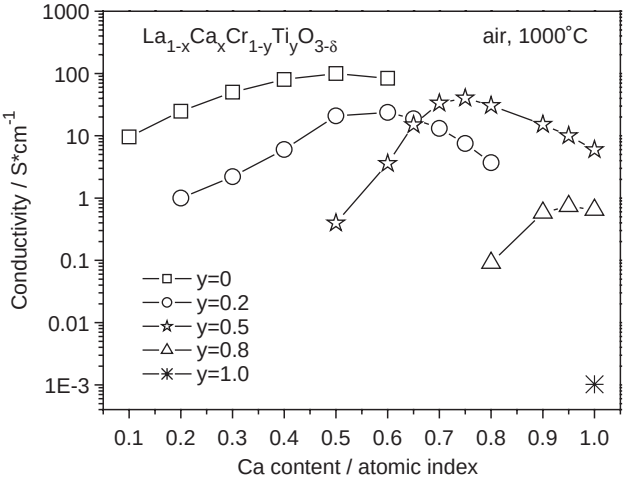

Fig. 9. Ca-content dependencies of the electrical conductivity of single-phase ceramics in the system $La_{1-x}Ca_xCr_{1-y}Ti_yO_{3-\delta}$ with $y=0$, 0.2, 0.5, 0.8, 1.0 in air at 1000 °C.

chromium cations having different oxidation states ($Cr^{3+} - e^- \rightleftharpoons Cr^{4+}$) [36] at oxidizing conditions. Increasing Cr content in $La_{1-x}Ca_xCr_{1-y}Ti_yO_{3-\delta}$ with the same Ca content is accompanied with a corresponding increase in the electrical conductivity. The observed discrepancy for $La_{1-x}Ca_xCr_{0.5}Ti_{0.5}O_{3-\delta}$ in the Ca concentration range $x = 0.7-1.0$ is explained with different macrostructures of the ceramic samples in the separate series. With the exception of $La_{1-x}Ca_xTiO_{3-\delta}$, the maxima of conductivity correspond exactly with the molar ratio of $[Cr^{3+}]/[Cr^{4+}]=1$.

4. Conclusions

Single-phase compounds of the series $La_{1-x}Ca_xCr_{1-y}Ti_yO_3$ with the nominal compositions $y = 0$, $x = 0-0.5$; $y = 0.2$, $x = 0.2-0.8$; $y = 0.5$, $x = 0.5-1$; $y = 0.8$, $x = 0.6-1$ and $y = 1$, $x = 0.8-1$ were prepared in air at maximum temperatures of 1350 °C. Compositions with Ca concentrations outside these ranges were found to be heterogeneous. An extended solid solution $La_{(1-x'-y)}Ca_{(x'+y)}Cr^{IV}_{x'}Cr^{III}_{(1-x'-y)}Ti_yO_3$ ($0 \leqslant x' < 0.6-0.7$, $x \leqslant y = 0$) with the orthorhombic perovskite-like $GdFeO_3$-type structure (space group *Pbnm*) is formed in the quasi-ternary system $CaCr^{IV}O_3$–$CaTiO_3$–$LaCr^{III}O_3$ at these conditions. Lattice parameters and average interatomic distances of the samples within the solid solution region decrease linearly with increasing Ca content.

Oxygen stoichiometry and electrical conductivity were investigated as functions of composition, temperature and oxygen partial pressure. At 900 °C and oxygen partial pressure 10^{-15}–10^5 Pa, the $La_{1-x}Ca_xCr_{1-y}Ti_yO_3$ compounds with $x > y$ are *p*-type and with $x \leqslant y$ *n*-type semiconductors. The observed conductivity types of the compounds with $x > y$ and $x \leqslant y$ can be explained with increasing concentration of Cr^{4+} cations and decreasing concentration of Ti^{3+} cations at elevated oxygen partial pressures, respectively. The decrease of the Ti^{3+}-concentration in compounds with $x < y$ is accompanied with the simultaneous increase of cationic vacancies.

The conductivity of the series $La_{1-x}Ca_xCr_{1-y}Ti_yO_3$ in air correlates with the product of the concentrations of Cr^{3+} and Cr^{4+}, if the oxidation numbers of La, Ca, Ti and O are assumed to be 3+, 2+, 4+ and 2−, respectively. Lanthanum–calcium chromite ($La_{0.5}Ca_{0.5}CrO_3$) shows the highest conductivity in air at 900 °C. Lanthanum–calcium titanates with minimal La content show the highest conductivity in reducing conditions. Changing conductivity types correlate with structural peculiarities and charge compensation mechanisms, which follow from the results of structural analysis.

Acknowledgment

The authors gratefully acknowledge the financial support of Deutsche Forschungsgemeinschaft (project GU 484/1-3) and the Ukrainian Ministry of Sciences (Projects "Cation" and DK-85-2003).

References

[1] R.T. Baker, I.S. Metacalfe, Appl. Catal. A 126 (1995) 297.
[2] J. Sfeir, J. van Herle, A.J. McEvoy, in: Ph. Stevens (Ed.), Proceedings of the Third European Solid Oxide Fuel Cells Forum, 2–5 June 1998, Nantes-France, pp. 267–273.
[3] P. Vernoux, M. Guillodo, J. Fouletier, A. Hammou, Solid State Ionics 135 (2000) 425.
[4] P.R. Slater, J.T.S. Irvine, Solid State Ionics 120 (2000) 125–134.
[5] A. Kaiser, J.L. Bradley, P.R. Slater, J.T.S. Irvine, Solid State Ionics 135 (2000) 519.

[6] O. Porat, C. Heremans, H. Tuller, J. Am. Ceram. Soc. 80 (1997) 2278.
[7] A. Hartley, M. Sahibzada, M. Weston, I.S.D. Metcalfe, Catal. Today 55 (2000) 197.
[8] M. Weston, I.S. Metcalfe, Solid State Ionics 113–115 (1998) 247.
[9] P. Karen, T. Norby, J. Electrochem. Soc. 145 (1998) 264.
[10] G. Pudmich, B.A. Boukamp, M. Gonzalez-Cuenca, W. Jungen, W. Zipprich, F. Tietz, Solid State Ionics 135 (2000) 433.
[11] M. Mogensen, N.M. Sammes, G.A. Tompsett, Solid State Ionics 129 (2000) 63.
[12] S. Tanasescu, D. Berger, D. Neiner, N.D. Totir, Solid State Ionics 157 (2003) 365.
[13] B.K. Flandermeyer, M.N. Nasrallah, A.K. Agarwal, H.U. Anderson, J. Am. Ceramic Soc. 67 (1984) 195.
[14] D.P. Karim, A.D. Aldred, Phys. Rev. B 20 (1979) 2255.
[15] I. Yasuda, M. Hishinuma, Solid State Ionics 80 (1995) 141.
[16] D.-H. Peck, M. Miller, K. Hilpert, Solid State Ionics 143 (2001) 401.
[17] B.A. van Hassel, T. Kawada, N. Sakai, H. Yokokawa, M. Dokiya, Solid State Ionics 66 (1993) 41.
[18] O.A. Marina, N.L. Canfield, J.W. Stevenson, Solid State Ionics 149 (2002) 21.
[19] H. Mitchell, A.R. Chakhmouradian, J. Solid State Chem. 144 (1999) 81.
[20] B.J. Kennedy, C.J. Howard, G.J. Thorogood, M.A.T. Mestre, J.R. Hester, J. Solid State Chem. 155 (2000) 455.
[21] G. Li, X. Kuang, Sh. Tian, F. Liao, X. Jing, Y. Uesu, K. Kohn, J. Solid State Chem. 165 (2002) 381.
[22] K.P. Bansal, S. Kumari, B.K. Das, G.C. Jain, J. Mater. Sci. 18 (1983) 2095.
[23] S.F. Palguev, V.K. Gilderman, V.I. Zemtzov, High Temperature Oxide Electronic Conductors for the Electrochemical Devices, Nauka, Moscow, 1990, 197p.
[24] V. Vashook, L. Vasylechko, U. Guth, H. Ullmann, Solid State Ionics 158 (2003) 317.
[25] V. Vashook, L. Vasylechko, U. Guth, H. Ullmann, Solid State Ionics 159 (2003) 279.
[26] V. Vashook, L. Vasylechko, U. Guth, H. Ullmann, J. Alloys Compds. 340 (2002) 263.
[27] V. Vashook, L. Vasylechko, U. Guth, H. Ullmann, J. Alloys Compds. 354 (2002) 13.
[28] L.G. Akselrud, P.Yu. Zavalij, Yu. Grin, V.K. Pecharsky, B. Baumgartner, E. Woelfel, Mater. Sci. Forum 133–136 (1993) 335.
[29] W. Gruner, Fres. J. Anal. Chem. 365 (1999) 597.
[30] K. Teske, H. Ullmann, N. Trofimenko, J. Thermal Anal. 49 (1997) 1211.
[31] M. Bode, K. Teske, H. Ullmann, GIT-Fachzeitschrift Lab 38 (1994) 495.
[32] V. Vashook, M. Al Daroukh, H. Ullmann, Ionics 7 (2000) 59.
[33] F. Lichtenberg, A. Herrnberger, K. Wiedenmann, J. Mannhart, Prog. Solid State Chem. 29 (2001) 1.
[34] J.B. Goodenough, et al., Mater. Res. Bull. 3 (1968) 471 (PDF2 21-137).
[35] I. Yasuda, M. Hishinuma Solid State Ionics 80 (1995) 141.
[36] P. Gerthsen, K.H. Härdtel, Z. Naturforschung 17a (1962) 514.